Effect of the order-disorder transition on the optical properties of Cu_2ZnSnS_4

M. Valentini,[1,2] C. Malerba,[1,3] F. Menchini,[1] D. Tedeschi,[2] A. Polimeni,[2] M. Capizzi,[2] and A. Mittiga[1,a)]
[1]*ENEA, Casaccia Research Center, via Anguillarese 301, 00123 Roma, Italy*
[2]*Department of Physics, University of Rome "Sapienza," P.le Aldo Moro 5, 00185 Roma, Italy*
[3]*DICAM, University of Trento, via Mesiano 77, 38123 Trento, Italy*

(Received 18 January 2016; accepted 17 May 2016; published online 26 May 2016)

The effect of the order-disorder transition on the band gap of kesterite Cu_2ZnSnS_4, an interesting material for solar cells, has been investigated by optical spectroscopy. The band gap energy (E_g) decreases continuously with increasing annealing temperature, T_a, and reaches its minimum at $T_a \sim 273\,^{\circ}C$. E_g is about 200 meV higher in the most ordered state, than in the fully disordered state. Its value and the transition kinetic depend on the sample stoichiometry. A simplified model able to explain the order degree and stoichiometry effects on the E_g value is developed. Ordering results in narrower Raman peaks without affecting the shape of the photoluminescence spectrum—except for the change in E_g—or the characteristic energy of the exponential tail below the fundamental absorption edge. Although a prolonged annealing increases the order degree, the material properties are still influenced by residual disorder as well as by defects related to the off-stoichiometry composition. *Published by AIP Publishing*. [http://dx.doi.org/10.1063/1.4952973]

Cu_2ZnSnS_4 (CZTS) is considered a good absorber material for thin film solar cells because it has a direct band gap of suitable value and is composed of abundant elements. However, solar cells based on CZTS have not yet got over the 10% efficiency barrier. One of the reasons for these unsatisfactory performances is the disorder in the distribution of Cu and Zn cations, which gives rise to band gap fluctuations that reduce carrier mobility and increase recombination. This disorder was first evidenced by X-ray and neutron diffraction experiments[1,2] and later by Nuclear Magnetic Resonance measurements[3] on CZTS samples cooled at different rates. In fast cooled samples, Cu and Zn atoms are randomly distributed in the (Cu,Zn) (001) planes while the Cu sites in the (Cu,Sn) (001) planes are occupied by Cu atoms only. The order degree in the (Cu,Zn) plane can be increased reducing the cooling rate as shown by near-resonant Raman studies,[4] where the ratio Q of the bands at 288 and 304 cm^{-1} was used as a rough estimate of the order parameter. Using Q it was found that the order-disorder transition is of the second order: above a critical temperature T_C ($\sim 260\,^{\circ}C$), the material is completely disordered while below T_C the equilibrium order degree increases gradually reaching the perfect order only at $T = 0\,K$.[4] The effect of disorder on the band gap, E_g, was investigated in CZTSe which exhibits a similar order-disorder transition ($T_C = 200\,^{\circ}C$).[5] It has never been studied, instead, in pure CZTS, the material object of the present investigation.

Two CZTS samples with comparable stoichiometry (see Table I) were obtained starting from two different precursors co-sputtered from CuS, SnS, and ZnS targets. The precursors were sulfurized for one hour at 550 °C in a tube oven under a Nitrogen/Sulfur atmosphere.[6]

The order degree of these two samples was modified by annealing treatments followed by quenching in water. After each annealing step, E_g was determined by transmittance at normal incidence (T) and absorptance (A) measurements. Absorptance was measured in the Edwards configuration[7] by placing the sample inside an integrating sphere. In this way, both transmitted and reflected light are collected, interference fringes are partially suppressed, and accurate A measurements are obtained even for A values as low as a few percent. In estimating the absorption coefficient α, multiple reflections inside the film were taken into account while interference effects were neglected, as described in Ref. 8. The α spectra were finally obtained by combining the values derived from A measurements for $\alpha < \alpha_0$ with those obtained from T measurements for $\alpha > \alpha_0$ (α_0 is a value for which the two curves overlap, typically in the range 5000–10 000 cm^{-1}). E_g values were derived from the plot of $(\alpha E)^2$ vs E (Tauc's plot).

The main aim of this work is to determine the E_g equilibrium values in a temperature range (160–320 °C) around that reported for the critical temperature ($T_C = 260\,^{\circ}C$).[4] First, two fully disordered samples were obtained by an annealing at 320 °C for 2 h followed by quenching in water. Then, the kinetic of the ordering transition was studied by three annealing processes at $T_a = 160$, 200, and 235 °C. In each process, the samples were exposed to successive isothermal annealing steps followed by quenching to room temperature and E_g measurements until the E_g equilibrium value was asymptotically approached. The results are shown in Fig. 1.

Sample K609 appears to reach equilibrium in a much faster way than sample K465. The samples were then

TABLE I. Samples' composition from EDX measurements.

Sample	[Cu] at. %	[Zn] at. %	[Sn] at. %	[S] at. %
K465	20.9	15.1	12.0	52.0
K609	19.8	16.2	11.6	52.4

a)Author to whom correspondence should be addressed. Electronic mail: alberto.mittiga@enea.it.

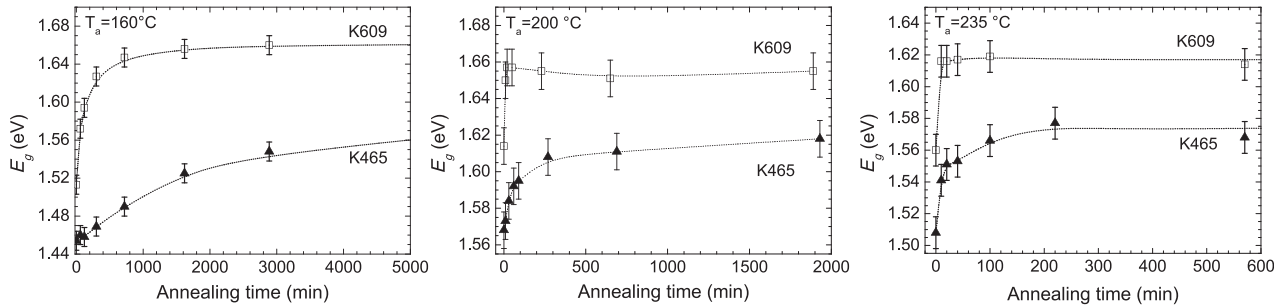

FIG. 1. Band gap change during ordering transitions at three annealing temperatures, $T_a = 160$, 200, and 235 °C for two CZTS samples. Dotted lines are guides to the eye.

brought to a high order level by a 24 h-long annealing at 160 °C followed by a very slow cooling (2 K/h) down to room temperature and energy gaps $E_g = 1.63$ eV and $E_g = 1.69$ eV were found for samples K465 and K609, respectively (not shown).

The dependence of E_g on T_a at equilibrium is then reported in Fig. 2. The first part of the equilibrium curve (disordering-cycle) was obtained by annealing the samples at increasing temperatures from 160 °C to 270 °C. Full equilibrium states at each temperature were reached by using dwell times, shown in the top of the figure, longer than the equilibration times found from the kinetic studies shown in Fig. 1. The samples were then annealed at 320 °C for 2 h to get a full disorder level. The second part of the equilibrium curve was then obtained by annealing the samples at decreasing temperatures (from 320 to 270 °C; ordering cycle).

The two E_g values found for $T_a = 270$ °C at the end of both the disordering and ordering cycles coincide within the experimental uncertainty, thus excluding hysteresis effects. The dependence of E_g on T_a shown in Fig. 2 is typical of a second order transition. The differences in the E_g absolute values and equilibration rates for the two samples should be likely ascribed to different sample stoichiometry, as will be discussed in the following.

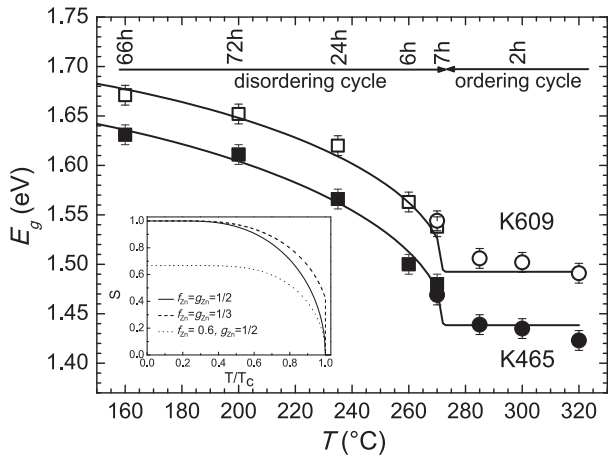

FIG. 2. Equilibrium values of the band-gap energy in two CZTS samples for different annealing temperatures. Annealing times at each T_a are reported on the top. Solid lines are fits of Eq. (6) to the data ($g_{Cu} = g_{Zn} = 1/2$, $T_C = 273$ °C, $E_{g0} = 1.59$ eV, $k = 0.3$ eV, [A] = 0.33 for sample K465 and [A] = 0.45 for sample K609). The inset shows numerical calculations of the order parameter S (Eq. (4)) as a function of T/T_C for $f_{Zn} = g_{Zn} = 1/2$ (solid line), for $f_{Zn} = g_{Zn} = 1/3$ (dashed line), and for ($f_{Zn} = 0.6$, $g_{Zn} = 1/2$) (dotted line).

The bandgap shift is not accompanied by a change in the characteristic energy E_T of the exponential tail below the fundamental absorption edge. E_T values are ~85 meV (see Fig. 3) and ~125 meV (not shown here) in samples K609 and K465, respectively. These high values agree with those (~80 meV) previously found by Photothermal Deflection Spectroscopy measurements in similar CZTS samples.[8]

Photoluminescence (PL) spectra of the sample K465 measured at 10 K in two different ordering states are shown in Fig. 4. PL intensity increases and PL bands blue shift with increasing ordering, in agreement with the literature.[9,10] It is interesting to note that the PL peak blue-shift (150 meV) nearly coincides with that of the band gap energy (160 meV) as determined by Tauc's plots of absorption coefficient. This observation is relevant to applications, because PL measurements can be easily performed in samples employed for device fabrication.

The effect of the order degree on the Raman spectrum has been investigated at room temperature (20 mW excitation at 532 nm, resolution 0.77 cm^{-1}; not shown here). The full width at half maximum of the main phonon mode, at ~338 cm^{-1}, is 5.6 cm^{-1} in the disordered state and 3 cm^{-1} in the ordered state, in good agreement with the literature.[9]

E_g equilibrium values have been tentatively analyzed by assuming[5] that E_g is a linear function of the long range order-parameter S which is obtained from kinetic

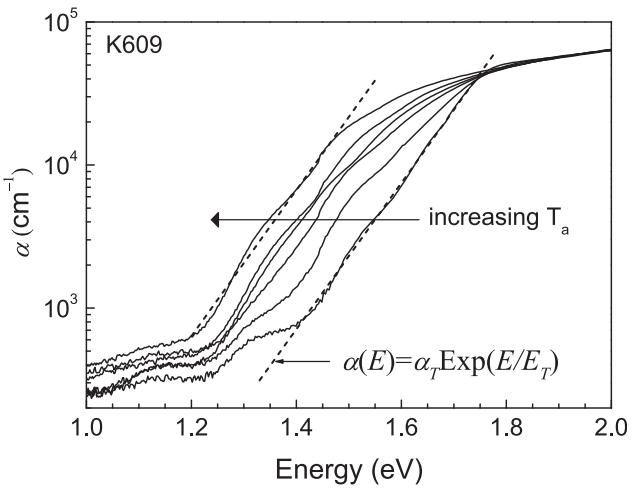

FIG. 3. Energy dependence of the optical absorption coefficient of sample K609 after annealing at different temperatures. Dashed lines are exponential fits to the absorption tails ($E_T = 85$ meV).

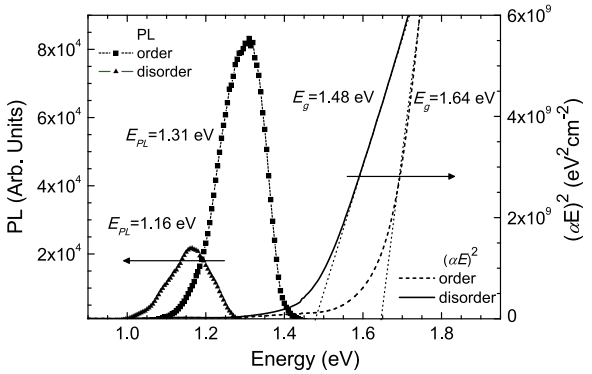

FIG. 4. Photoluminescence spectra of sample K465 at 10 K in two different ordering states. The corresponding Tauc's plots obtained from spectrophotometric measurements are also reported.

theories.[11,12] Following the chemical rate theory,[11] the theory for stoichiometric binary alloys[12] used in a previous work[5] is here generalized to non-stoichiometric binary sublattice by taking into account both the fraction of available sites in the crystal structure (g_{Cu} and g_{Zn}, with $g_{Zn}+g_{Cu}=1$) and the fraction of atoms (f_{Cu} and f_{Zn}, with $f_{Zn}+f_{Cu}=1$). Contrary to the atom fractions f_{Cu} and f_{Zn}, the fraction of sites for Cu (g_{Cu}) and Zn (g_{Zn}) do not depend on stoichiometry. In our case, g_{Cu} and g_{Zn} can reasonably assume only two pair of values: If Zn atoms can swap with any Cu atom, the crystal structure implies $g_{Cu}=2/3$ and $g_{Zn}=1/3$; if instead, the occupation of a Cu site in the Cu-Sn plane by a Zn atom has a high energy cost, Zn atoms remain in the Cu-Zn planes, the system is 2-dimensional, and the crystal structure implies $g_{Cu}=g_{Zn}=1/2$. The long range order parameter is defined as $S=(P(Cu_{Cu})-f_{Cu})/(1-f_{Cu})$, where $P(Cu_{Cu})$ is the probability to find a Cu atom on a Cu site. In a typical non-stoichiometric Cu-poor material ($f_{Cu}<g_{Cu}$), the perfect order ($S=1$) cannot be reached and S is limited to $S_{\max}=(f_{Cu}/g_{Cu}-f_{Cu})/(1-f_{Cu})=(f_{Cu}g_{Zn})/(f_{Zn}g_{Cu})$.

The kinetic of long range order parameter can be written as

$$\frac{dS}{dt}=\frac{1}{g_{Zn}}\left[K_O(1-S)(g_{Zn}f_{Cu}-f_{Zn}g_{Cu}S)-K_D\left(g_{Zn}(1-S)+S\right)\left(1-f_{Zn}(1-S)\right)\right]. \quad (1)$$

The ordering (K_O) and disordering (K_D) rates are given by

$$K_O=f\exp\left(-\frac{U}{kT}\right)\exp\left(\frac{V_0S}{2kT}\right),$$
$$K_D=f\exp\left(-\frac{U}{kT}\right)\exp\left(-\frac{V_0S}{2kT}\right). \quad (2)$$

U and f are the activation energy and the attempt frequency for the Cu-Zn exchange process in the fully disordered state. For $f_{Zn}=g_{Zn}$, Eq. (1) is equivalent to Eq. (16) reported in Ref. 12 that holds for stoichiometric compounds. The equilibrium value of S for any temperature below T_C can be found equating the right hand side of Eq. (1) to zero. This leads to

$$\frac{(g_{Zn}(1-S_{eq})+S_{eq})(1-f_{Zn}(1-S_{eq}))}{(1-S_{eq})(g_{Zn}f_{Cu}-f_{Zn}g_{Cu}S_{eq})}=\exp\left(\frac{V_0S_{eq}}{kT}\right). \quad (3)$$

For small enough values of S_{eq}, by approximating the exponential with a linear function and solving the equation for $S_{eq}=0$, one finds $T_C=(V_0f_{Zn}g_{Cu})/k$ and

$$\frac{(g_{Zn}(1-S_{eq})+S_{eq})(1-f_{Zn}(1-S_{eq}))}{(1-S_{eq})(g_{Zn}f_{Cu}-f_{Zn}g_{Cu}S_{eq})}=\exp\left(\frac{T_cS_{eq}}{f_{Zn}g_{Cu}T}\right). \quad (4)$$

For generic values of $S_{eq}(T)$, Eq. (4) must be solved numerically, as shown in the inset of Fig. 2 for three typical cases: $f_{Zn}=g_{Zn}=1/3$, $f_{Zn}=g_{Zn}=1/2$, and $f_{Zn}=0.6$, $g_{Zn}=1/2$.

For $g_{Zn}=1/3$, the order parameter exhibits a first order phase transition with a large discontinuity at T_C, which is not compatible with the behavior observed here for the energy gap. Therefore, $g_{Zn}=1/2$ will be assumed in the following, in agreement with the previous observations.[1–3] Finally, the case $f_{Zn}=0.6$ and $g_{Zn}=1/2$ highlights the limitation in the maximum S value due to an off-stoichiometry composition (Zn-rich).

The simplest correlation between E_g and S that may account for the effect of the non-stoichiometry is now searched for. Our films as well as all CZTS films used in good devices are characterized by a Zn-rich and Cu-poor stoichiometry and by a low hole density which implies that their large non-stoichiometry is accommodated by high concentrations of neutral $[Zn_{Cu}^{+}+V_{Cu}^{-}]$ pairs (A defects) and $[2Zn_{Cu}^{+}+Zn_{Sn}^{2-}]$ pairs (B defects).[13] The effect on the material band gap of high concentrations of those defect complexes as well as that of $[Zn_{Cu}^{+}+Cu_{Zn}^{-}]$ antisite pairs (P defects, hereinafter) has been investigated by *ab-initio* calculations.[10,14–17] Despite those theoretical results only partially agree, they all conclude that the A defects widen the gap, P defects shrink the gap, and B defects lead to a very small (or null) decrease of the gap. Furthermore, it has been suggested that the combined effect of an A and a P defect does not change the gap.[15] Therefore, the following simplified linear relationship between complex concentrations and E_g is proposed:

$$E_g=E_{g0}+k([A]-[P]), \quad (5)$$

where the complex concentrations are expressed as the average number of complexes in a conventional 16-atom kesterite unit cell.[10] In a stoichiometric CZTS and assuming that the exchange between Cu and Zn takes place only in the (Cu,Zn) planes ($f_{Zn}=g_{Zn}=1/2$), the definition of S implies $[P]=1-S$. Therefore, k is the gap difference between a fully ordered ($[P]=0$) and a completely disordered ($[P]=1$ which corresponds to a complex density of 3.12×10^{21} cm^{-3}) material. In the general case, by following the same approach used to derive Eq. (1), [P] can be written as

$$[P]=2P(Cu_{Zn})=2\left(f_{Cu}-\frac{f_{Zn}}{g_{Zn}}g_{Cu}S\right), \quad (6)$$

where the factor 2 is introduced because the conventional unit cell contains two Zn sites. Notice that for $S=S_{max}=(f_{Cu}g_{Zn})/(f_{Zn}g_{Cu})$, Eq. (6) gives $[P]=0$ and the Zn_{Cu} antisites will be due only to A or B defects. Equation (5) can be fitted to the experimental data by using Eqs. (1) and (4)

TABLE II. Stoichiometry values deduced from the [A] values obtained from *Eg* fits.

Sample	[Cu] at. %	[Zn] at. %	[Sn] at. %	[S] at. %
K465	21.2	15.0	12.8	51.0
K609	20.0	15.7	12.9	51.4

provided [A], g_{Zn}, and f_{Zn} have reasonable values. While the gradual change in E_g leads to assume $g_{Zn} = 1/2$, the values of [A] and f_{Zn} require an accurate knowledge of the material's chemical composition. This is hampered by the uncertainty in the Energy Dispersive X-ray spectroscopy (EDX) measurements and the presence of small grains of spurious phases (mainly ZnS) that form during the sulfurization process. However, a correlation between f_{Zn} and [A] is established by the preferential location of copper vacancies in the (Cu,Sn) planes[13] and the excess zinc in the (Cu,Zn) planes.[1–3] In a material without B-type defects, this correlation can be expressed as

$$f_{Zn} = \frac{[Zn_{2d}]}{[Zn_{2d}] + [Cu_{2c}]} = \frac{2 + [A]}{2 + [A] + 2 - [A]} = \frac{1}{2} + \frac{[A]}{4}. \quad (7)$$

Therefore, the E_g data shown in Fig. 2 have been tentatively fitted by assuming a non-stoichiometry due to A defects only. A good agreement with the experimental data has been achieved using $T_C = 273\,^{\circ}\mathrm{C}$, $E_{g0} = 1.59\,\mathrm{eV}$, $k = 0.3\,\mathrm{eV}$, and by taking $[A] = 0.33$ (namely, $f_{Zn} = 0.58$) for sample K465 and $[A] = 0.45$ ($f_{Zn} = 0.61$) for sample K609 (solid lines in Fig. 2). These values of [A] correspond to the stoichiometry values reported in Table II: we can see that they are compatible with the values measured by EDX (see Table I) within the errors.

The interpretation of the kinetic data is more difficult. Eq. (1) predicts a sigmoidal shape of $S(t)$, with $d^2S/dt^2 > 0$ until S reaches about half of its asymptotic value. From Eqs. (5) and (6) this behavior should be observed in the time dependence of E_g also.

The experimental data, instead, show a fast initial rise followed by a slower approach toward equilibrium. Most likely, this disagreement is due to the neglect of the short range ordering effects by the kinetic theories[11,12] used here and in all previous works.[4,5] These theories are based on the strong approximation of a completely uncorrelated occupation of the lattice sites and therefore neglect short range order as well as nucleation, growth, and coalescence of domains of order. This approximation, which is justified for $S > 0.5$, progressively loses validity in more disordered states.[12] The annealing data at 160 °C of sample K609 clearly show this problem as they cannot be fitted by the solution of Eq. (1). Therefore, the transients have been approximately fitted with a single exponential (see Fig. 5). The obtained time constants τ_{ord} are reported in Table III together with the results obtained from an Arrhenius plot ($\tau_{ord} = \tau_0 \exp(-E_A/kT)$) for sample K465 (the fast kinetic of K609 did not allow to obtain a meaningful fit at 235 C).

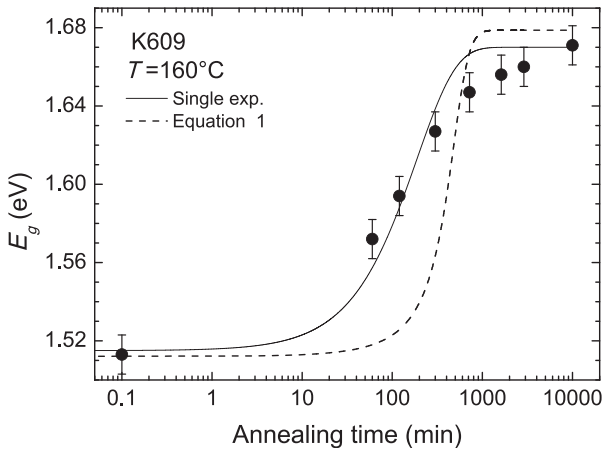

FIG. 5. Fits of different models to the equilibration transient data of sample K609 at 160 °C are shown in Fig. 1. The last point is the saturation value of the energy gap obtained from the study of the equilibrium value of E_g. It has been arbitrarily located at $t = 10^4$ min to allow its visualization on the graph.

TABLE III. τ_{ord}, activation energy E_A, and τ_0 from an exponential fit of the ordering transients.

Sample	τ_{ord} (160 °C) (min)	τ_{ord} (200 °C) (min)	τ_{ord} (235 °C) (min)	E_A (eV)	τ_0 (s)
K465	3276	89	17	1.34	4.1×10^{-11}
K609	188	4	<2	…	…

The obtained E_A value, though derived by such a rough analysis, is not unreasonable for an energy barrier ruling a Cu-Zn exchange process. Further investigations are required to clarify possible correlations between ordering kinetic and sample stoichiometry.

In conclusion, we have shown that the gap of CZTS is susceptible to large variations (~0.3 eV) as a consequence of ordering and changes in sample stoichiometry. The Vineyard model generally used to describe the order-disorder transition has been generalized to non-stoichiometric compounds. The use of this improved model suggests that, beside the well accepted decrease in E_g caused by increasing disorder, another part of the gap variability is due to the different concentrations of A-type defects, which tend to increase the gap. Furthermore, experimental data on the ordering kinetic have been presented and very different results have been found in two samples with different compositions. Understanding the factors which are able to speed up the ordering kinetic could help to obtain CZTS films with a higher order level.

This work was partially supported by the Italian Ministry of Economic Development in the framework of the Operating Agreement with ENEA for the Research on the Electric System.

[1]S. Schorr, Thin Solid Films **515**, 5985 (2007).
[2]S. Schorr, Sol. Energy Mater. Sol. Cells **95**, 1482 (2011).
[3]L. Choubrac, M. Paris, A. Lafond, C. Guillot-Deudon, X. Rocquefelte, and S. Jobic, Phys. Chem. Chem. Phys. **15**, 10722 (2013).
[4]J. J. S. Scragg, L. Choubrac, A. Lafond, T. Ericson, and C. Platzer-Bjorkman, Appl. Phys. Lett. **104**, 041911 (2014).
[5]G. Rey, A. Redinger, J. Sendler, T. P. Weiss, M. Thevenin, M. Guennou, B. El Adib, and S. Siebentritt, Appl. Phys. Lett. **105**, 112106 (2014).
[6]M. Valentini, C. Malerba, E. Salza, M. De Luca, M. Capizzi, and A. Mittiga, in *IEEE 40th Photovoltaic Specialist Conference, PVSC 2014* (2014), p. 439.
[7]G. Owen, Rev. Sci. Instrum. **68**, 1369 (1997).

[8]C. Malerba, F. Biccari, C. L. Azanza Ricardo, M. Valentini, R. Chierchia, M. Muller, A. Santoni, E. Esposito, P. Mangiapane, P. Scardi, and A. Mittiga, J. Alloys Compd. **582**, 528 (2014).
[9]M. Grossberg, J. Krustok, T. Raadik, M. Kauk-Kuusik, and J. Raudoja, Curr. Appl. Phys. **14**, 1424 (2014).
[10]J. J. S. Scragg, J. K. Larsen, M. Kumar, C. Persson, J. Sendler, S. Siebentritt, and C. Platzer-Bjorkman, Phys. Status Solidi B **253**, 247 (2016).
[11]G. J. Dienes, Acta Metall. **3**, 549 (1955).
[12]G. H. Vineyard, Phys. Rev. **102**, 981 (1956).
[13]A. Lafond, L. Choubrac, C. Guillot-Deudon, P. Deniard, and S. Jobic, Z. Anorg. Allg. Chem. **638**, 2571 (2012).
[14]J. Paier, R. Asahi, A. Nagoya, and G. Kresse, Phys. Rev. B **79**, 115126 (2009).
[15]D. Huang and C. Persson, Thin Solid Films **535**, 265 (2013).
[16]S. Chen, A. Walsh, X. G. Gong, and S. H. Wei, Adv. Mater. **25**, 1522 (2013).
[17]W. Xiao, J. N. Wang, X. S. Zhao, J. W. Wang, G. J. Huang, L. Cheng, L. J. Jiang, and L. G. Wang, Sol. Energy **116**, 125 (2015).